NATIONAL ADVISORY COMMITTEE FOR AERONAUTICS

TECHNICAL NOTE 3396

ICING LIMIT AND WET-SURFACE TEMPERATURE VARIATION FOR TWO AIRFOIL SHAPES UNDER SIMULATED HIGH-SPEED FLIGHT CONDITIONS

By Willard D. Coles

Lewis Flight Propulsion Laboratory
Cleveland, Ohio

Washington
February 1955

NATIONAL ADVISORY COMMITTEE FOR AERONAUTICS

TECHNICAL NOTE 3396

ICING LIMIT AND WET-SURFACE TEMPERATURE VARIATION FOR TWO AIRFOIL SHAPES UNDER SIMULATED HIGH-SPEED FLIGHT CONDITIONS

By Willard D. Coles

SUMMARY

Frictional heating resulting from flight at high speeds effectively reduces the value of ambient-air temperatures at which ice forms on aircraft surfaces. An experimental study was made of the wet-surface temperature and the stream conditions that result in ice-free surfaces for bodies in flight through icing clouds, and the results obtained are compared with values calculated using an analytical method. Two symmetrical airfoil models, one of diamond shape and the other of double-circular-arc contour, were used in the investigation. Results are presented for Mach numbers from 0.6 to 1.35 and for pressure altitudes from 25,000 to 40,000 feet.

The experimental investigation gave values of the wet-surface temperature that were consistently 2° to 4° F higher than the values calculated by the analytical method for all but the foremost part of the airfoils. The analytical method gave conservative results, compared with the experimental results, predicting the initial formation of ice to occur at values of ambient-air temperature up to 12° F higher than were found experimentally. The experiments generally substantiated the analytically determined location of critical regions on the bodies for the initial formation of ice and provided sufficient agreement with analytical results to prove their validity.

INTRODUCTION

As flight speeds are increased into the transonic and supersonic regimes, the frictional heating of aircraft surfaces becomes of considerable importance in reducing the susceptibility of the surfaces to icing. Atmospheric conditions that are regarded as extremely hazardous icing conditions for low-speed aircraft may be completely harmless at higher flight speeds. The set of flight conditions providing a surface temperature of 32° F for a particular point on a body running fully wet in an

icing cloud is termed the icing limit for that point in references 1 and 2. The analysis presented in reference 1 equates the frictional heating term to the evaporative and heat-transfer terms in a heat balance for the icing-limit condition for a diamond airfoil in transonic and supersonic flight. The results of reference 1 show that a critical region for the initial formation of ice exists at or just behind the shoulder of the diamond airfoil as a result of the reduced pressure and consequent increase in the evaporative cooling effect in this region. A limited experimental verification of the results of the analysis of reference 1 was also presented therein.

The procedure used for calculating the icing limit in reference 1 was applied generally in reference 2 to obtain charts that would facilitate the determination of the icing limit at any point on a body in terms of the stream conditions. Because certain of the conditions and assumptions made in the analysis were not known to be fully applicable at high flight speeds, an experimental investigation of the icing limit was made and is reported herein. Two airfoil shapes, a symmetrical diamond airfoil and a symmetrical circular-arc airfoil, were investigated over a Mach number range of from 0.6 to 1.35 and for pressure altitudes from 25,000 to 40,000 feet. This investigation was conducted in a 3.84- by 10-inch tunnel at the NACA Lewis laboratory.

SYMBOLS

The following symbols are used in this report:

C_p pressure coefficient, $\frac{p_1 - p_0}{\frac{1}{2}\rho_0 V_0^2}$

c_p specific heat of air at constant pressure, (0.24) Btu/(lb)($^\circ$F)

D diffusivity of vapor in air, sq ft/sec

e vapor pressure, lb/sq ft

g acceleration due to gravity, ft/sec^2

k thermal conductivity of air, Btu/(sec)(sq ft)($^\circ$F/ft)

k_e coefficient of evaporation

k_h coefficient of transfer of heat

L latent heat of vaporization, 1075.8 Btu/lb at 32° F

M	Mach number
m_a	molecular weight of air
m_e	molecular weight of water vapor
Pr	Prandtl number, $= \frac{c_p \mu g}{k}$
p	static pressure, lb/sq ft (sum of dry-air and water-vapor partial pressures)
r	recovery factor from $T_{ad,w} = T_0\left[1 + \frac{r(\gamma-1)}{2} M_1^2\right]$
T	static temperature, $^{\circ}R$
$T_{ad,w}$	adiabatic wall temperature, $^{\circ}R$
$T_{0,c}$	minimum free-stream static temperature corresponding to ice-free condition on surface, $^{\circ}R$
Tr	Taylor number $= \frac{\mu}{\rho D}$ = Schmidt number
t	temperature, $^{\circ}F$
V	velocity, ft/sec
x/c	chordwise position (distance from leading edge divided by chord length)
γ	ratio of specific heats of air = 1.400
μ	viscosity of air, slugs/(ft)(sec)
ρ	density of air, slugs/cu ft

Subscripts:

s	surface
0	free-stream conditions
1	local conditions at edge of boundary layer

ANALYSIS

The generalized heat balance for a thermally insulated body moving relative to an icing cloud is given in references 1 and 2 as follows:

(1) Heat due to frictional effects

plus

(2) Heat due to kinetic energy of water droplets

plus

(3) Heat of fusion

equal

(4) Heat lost by convection

plus

(5) Heat for evaporation of water

plus

(6) Heat required to raise temperature of impinging water from stream temperature to surface temperature

The analytical results of references 1 and 2 are based on the use of Hardy's relation (ref. 3), which is obtained by equating the frictional term (1) to the sum of the convective term (4) and the evaporative term (5). The heat of fusion term (3) is equal to zero if no ice is forming on the surface or in the water film. Thus, at the icing limit, for Hardy's relation to be valid term (2) must be nearly equal to term (6) or the difference between the two terms must be small compared with term (1). Both terms (2) and (6) are functions of the liquid-water content of the cloud, and, for values of liquid-water content usually associated with high-speed and thus high-altitude flight, both the terms are quite small and of nearly the same magnitude. The difference between the values of terms (2) and (6) is less than 3 percent of term (1) for the following severe flight conditions: Mach number, 1.36; pressure altitude, 35,000 feet; ambient-air temperature, -30° F; and liquid-water content, 0.5 gram per cubic meter.

The relation of Hardy given in references 1 and 2 is

$$T_s = T_1\left[1 + \frac{r(\gamma-1)}{2} M_1^2\right] - \frac{k_e}{k_h}\frac{m_e}{m_a}\frac{L}{c_p}\left(\frac{e_s}{p_1 - e_s} - \frac{e_1}{p_1 - e_1}\right) \qquad (1)$$

The ratio of the evaporation coefficient k_e to the heat-transfer coefficient k_h is usually accepted (refs. 1 to 3) as having a value nearly equal to unity for water evaporating into air at temperatures near 32° F. For laminar flow, the relation is given in reference 3 as $k_e/k_h = (Pr/Tr)^{2/3}$. Numerical evaluation of this relation yields a value of approximately 1.10. For turbulent flow, an analytical treatise (ref. 4) indicates the value of the ratio to be approximately 1.05. An experimental investigation of the sublimation of ice (ref. 5) gives a value of 0.90 for the ratio. Because of the uncertainty of the value of the ratio, a value of unity, which represents an average, was used in accord with that used in references 1 and 2. In addition, if, as assumed in references 1 to 3, the flow about the body outside the boundary layer is accomplished with no change in phase of the vapor or droplets, then Dalton's law of partial pressures applies and $e_1/e_0 = p_1/p_0$, and in equation (1) $e_0/(p_0 - e_0)$ may be substituted for $e_1/(p_1 - e_1)$.

For purposes of calculation and presentation of the results, equation (1) is put in the following form:

$$492 = T_1 \frac{\left(1 + \frac{\gamma-1}{2} rM_1^2\right)}{T_{0,c}} T_{0,c} - 2788.6 \frac{12.75}{\left(\frac{p_1}{p_0}\right) p_0 - 12.75} - \frac{e_0}{p_0 - e_0} \qquad (2)$$

This is the equation of reference 2 with a slightly different value of the constant. The icing-limit temperature (free-stream static temperature, $T_{0,c}$) was determined in reference 2 as a function of the parameters $\left(T_1/T_{0,c}\right) \times \left(1 + \frac{\gamma-1}{2} rM_1^2\right)$ and p_1/p_0 for altitudes from sea level to 45,000 feet, the maximum probable icing-cloud altitude. In addition, charts were presented for the rapid determination of the parameter $\left(T_1/T_{0,c}\right) \times \left(1 + \frac{\gamma-1}{2} rM_1^2\right)$ from the stream and flow conditions about a body.

The experimental investigation of the icing limit consisted essentially in determining the value of the stream static temperatures at which ice would first start to form on, or just be removed from, a surface in a high-velocity air stream. For this purpose, a symmetrical diamond airfoil and a symmetrical circular-arc airfoil, each having a chord length of 6 inches and a thickness-to-chord ratio of 6 percent, were used in the study. Both airfoil models were made of brass and were provided with 11 static-pressure taps in the chordwise direction. A transparent plastic insert, which formed a relatively large (1 by 5 in.) portion of the central part of each airfoil, provided an insulated region free from conduction effects where local surface temperatures could be

determined. The ratio of the thermal conductivity of the plastic insert to that of the rest of the model was approximately 2.5×10^{-3}. Fifteen thermocouples were located in the surface of the plastic in a chordwise direction parallel to the static taps. A photograph of the circular-arc airfoil model showing the static taps, the plastic insert, and the thermocouples is presented in figure 1. The diamond airfoil was of similar construction.

A schematic diagram of the 3.84- by 10-inch tunnel in which the experiments were conducted is shown in figure 2. One wall of the test section was of glass for the purpose of observing the formation of ice on the airfoil models. Permanent instrumentation of the tunnel includes static-pressure taps along the top and bottom walls of the tunnel and pressure taps and thermocouples in the plenum chamber. The airfoil models were mounted on a porthole in the tunnel wall that was also provided with static-pressure taps.

The air for the tunnel was provided from a central supply system at the following initial conditions: pressure, 10 pounds per square inch gage; temperature, -20° F; and humidity ratio, approximately 3.0×10^{-4} pounds of water vapor per pound of dry air. By means of electric and steam heaters and a control valve at the inlet to the plenum chamber, the air was conditioned to the desired values of temperature and pressure at the tunnel test section.

A sensitive dewpoint meter was used to determine the frostpoint temperature of a continuous sample of air from the tunnel plenum chamber.

An air-atomizing spray nozzle, located approximately 18 inches upstream of the model as shown in figure 2, was used to provide local values of the liquid-water content of the air from 0.5 to 7.0 grams per cubic meter at the model. The liquid-water content of the air was estimated from measured values of water-flow rate together with determinations of the volume flow of air through the observed area of spray coverage. The volume-median drop size was estimated to be approximately 15 microns from previous experiments with dimensionally similar nozzles in the 6- by 9-foot icing research tunnel. A calculated value for the mean droplet diameter of approximately 18 microns was obtained using the conditions of the experiments in an empirical equation of Nukiyama and Tanasawa (ref. 6).

METHOD AND PROCEDURE

The icing limit has been defined as "the set of flight conditions which provides a [wet and ice free] surface temperature of 32° F for a particular point on a body traveling in an icing cloud" (ref. 2). The general equation (1) does not include the 32° F surface temperature

restriction, and can be checked at other temperatures. The specific application of the general equation to the icing limit adds no complication, except that, for the experimental investigation, a slight amount of ice must form to enable the determination of the icing limit. Thus, experimentally the release of the heat of fusion of a small amount of ice occurs but is negligible and is not considered in the analysis.

The experimental procedure consisted in operating the tunnel at constant conditions of pressure altitude, Mach number, and free-stream vapor concentration, while the temperature of the air at the plenum chamber was controlled to achieve the desired temperature conditions at the model. Measurements of surface temperature were obtained for both the wet and dry surface conditions. The dry surface temperature measurements were taken in order to obtain values of the recovery factor used in equation (1). The experimental value of the icing limit was determined for each Mach number and pressure altitude condition by first selecting a value of plenum air temperature for which ice would form on the model, and gradually increasing the temperature until the ice would no longer form. No appreciable accumulation of ice was allowed to form on the model, as the local pressure changes caused by the rough ice are conducive to the formation of more ice, and the formation of more than minute quantities of ice would require that the heat of fusion be considered in the investigation. The value of the plenum temperature that corresponds to the icing-limit conditions was then used to determine the value of free-stream static temperature on the basis of a dry-air adiabatic process to be compared with the analytical results of references 1 and 2.

RESULTS AND DISCUSSION

Several factors influenced the size requirements considered in the design of the airfoil models used for the investigation. Problems arising from the model instrumentation and mounting of the models in the tunnel so that icing of mounting devices would not be a source of difficulty required that the models be of relatively large size. However, at high air velocities, an effect on the flow field about the model results if the ratio of model-to-tunnel cross-sectional dimensions is large. As measured values of the local static pressures were to be used in the determination of the icing-limit conditions, it was not necessary, however, that the flow field about the model be completely free from tunnel wall effect; and, therefore, some design compromise was possible in the size of the models.

Chordwise Variation of Pressure Distribution

Pressure distributions on the models for $M_0 = 1.35$ are shown in figure 3. The pressure coefficient C_p is presented as a function of

the chord position for the two models, and corresponding theoretical relations are presented for comparison. The leading-edge shock wave is reflected by the tunnel walls and intersects the models at approximately the 70-percent-chord position. The effect on the local static pressure is quite severe in the vicinity of and behind the shock-wave intersection. Some data obtained in this region are included throughout the report to show the results of this disturbance in the flow field on the surface temperature.

Chordwise Variation of Recovery Factor

In order to calculate icing-limit temperatures, a reasonably accurate value for the recovery factor r must be used in equation (1). The recovery factor is a function of the body shape and also depends upon whether the flow is laminar or turbulent. For usual body shapes, the value of the recovery factor is between 0.84 (laminar) and 0.90 (turbulent) (ref. 7). The extremes of this variation are sufficient to change the value of the icing limit determined from equation (1) by several degrees Fahrenheit. Therefore, values of the recovery factor for each of the airfoil models were experimentally determined for subsonic and supersonic conditions over a range of pressure altitude. Both local surface temperature and local Mach number values are required for the determination of the recovery factor. As the chordwise position of the thermocouples and pressure taps did not exactly coincide, values of surface temperature corresponding to the static-tap location were obtained from plots of surface temperature against chordwise position. Thus, the recovery-factor values correspond to the chordwise location of the static taps on the model. The use of faired values of surface temperature gave more accurate results than could be obtained with faired values of static pressure or local Mach number, because the number of thermocouples was greater than the number of static-pressure taps.

Figure 4 shows recovery factor as a function of the chordwise position for the diamond airfoil model at values of the free-stream Mach number of 0.8 and 1.35. At the lower Mach number condition (fig. 4(a)), the value of the recovery factor was approximately 0.86 over the front half of the model and 0.87 over the rear half. For the supersonic case (fig. 4(b)), the value of the recovery factor was higher, averaging slightly greater than 0.88 over the front surface and approximately 0.89 for the rear surface.

Values of the recovery factor obtained with the circular-arc airfoil at Mach numbers of 0.6, 0.8, and 1.35 at 30,000-feet pressure altitude are shown in figure 5(a). The recovery factor shows a slightly higher value at the higher Mach numbers. Figure 5(b) presents the circular-arc-airfoil recovery factor for a Mach number of 1.35 for pressure altitudes from 25,000 to 40,000 feet. Figures 4(a) and (b) and 5(b) show that, for

both the diamond and the circular-arc airfoils, the effect of increasing air density (decreasing pressure altitude) on the value of the recovery factor is similar to the effect of increasing Mach number, and both might thus be described as Reynolds number effects. However, for the Reynolds number range of this investigation almost the entire chord length of the airfoil is in the transition region from laminar to turbulent flow, and any increase in Reynolds number results in a more turbulent regime with consequent increase in the recovery factor.

The recovery factor obtained when the occurrence of fully turbulent flow is accelerated by roughness near the leading edge is shown in figure 5(c). A band of number 80 grit, 3/16 inch wide, was cemented to the model just behind the leading edge to promote the increased turbulence. The recovery factor behind the roughened surface is 0.87 at the first point of measurement, as compared with 0.845 obtained with the smooth surface. The increase in recovery factor due to roughness diminishes as a function of the distance from the leading edge, showing that almost fully turbulent flow exists at the midchord position without roughness.

The recovery factor can be determined only for a dry surface; therefore, the effect of a surface water film cannot be evaluated, but should be of no greater magnitude than that experienced with the leading-edge roughness. For both the diamond and circular-arc airfoils, a value of 0.88 for the recovery factor would seem to be applicable for conditions involving some roughness due to water film or ice for all but the very foremost regions of the airfoils.

Diamond Airfoil

Surface temperature and icing limit - rear surface. - The existence of a critical region for the formation of ice just behind the shoulder of the diamond airfoil was predicted and experimentally substantiated in reference 1. A similar result was experienced during the present investigation, and a photograph of ice formed on the rear surface of the airfoil model is shown in figure 6. Conduction of heat from the tunnel walls and from the unwetted regions of the brass portion of the model prevented the formation of ice on any part of the model except the plastic insert and areas immediately adjacent.

Experimental values of the wet-surface temperature behind the shoulder were often not obtained, because as the water film flowed over the shoulder it divided into rivulets that frequently missed the thermocouples entirely.

For both the diamond and circular-arc airfoil models, the experimental and analytical results could be evaluated in two ways. First, the temperature and flow conditions that would result in the first slight

formation of ice at a point on the surface of the model were experimentally determined, from which the value of the free-stream static temperature t_0 was determined from compressible flow relations. Analytical values of the free-stream static temperature $t_{0,c}$ from reference 2 (whenever applicable), which were also determined for the local conditions corresponding to the location of the ice formation, are presented with the experimental values in the figures. In addition, for each of the icing-limit conditions, the measured surface temperatures obtained over the model are presented, together with curves showing the surface temperature variation calculated with equation (1) for each point of measurement of local static pressure on the model, with the value of t_0 determined from the experiments assuming a dry adiabatic process.

Measured surface temperature values obtained at $M_0 = 0.8$ for two values of pressure altitude are shown in figures 7(a) and (b) for the icing-limit condition (stream temperature for which ice just starts to form). Included also are the calculated surface temperature (eq. (1)) and the location of the ice formation in terms of chordwise position. A value of 0.88 was used for the recovery factor in making the calculations. A fully wetted surface condition prevails over the front face of the diamond airfoil, and the calculated surface temperature curve closely approximates the measured values. In the region near the leading edge, the use of a lower value of the recovery factor would result in closer agreement with the measured values.

The critical region at the shoulder is highly localized in the case of the subsonic free-stream condition, and conduction of heat from other parts of the model would tend to limit the temperature reduction in this region. The conduction effect could thus be partly responsible for the fact that, at the value of free-stream static temperature for which ice just began to form on the airfoil (surface temperature of 32° F at shoulder), the value of the calculated surface temperature was somewhat below the freezing level. In general, values of calculated surface temperature below 32° F do not have much significance other than to indicate the location of an ice-formation region; and, therefore, the curves are shown as dashed lines below 32° F. For equation (1) to be applicable, the surface must be ice-free; and, therefore, values of the calculated surface temperature below the freezing level indicate the temperature that supercooled water would assume if it existed on the surface.

High values of the measured surface temperature behind the shoulder result from the rivulet nature of the runback water flow, the surface being only partly wet. In general, the thermocouples that were observed to be wetted by a rivulet reached an equilibrium wet-surface temperature that was unchanged by increasing the water flow. For the subsonic part of the experimental investigation, the free-stream humidity was considerably below the saturation value for the stream static temperature. Therefore, no direct comparison of the free-stream static temperature for the

icing-limit condition can be made with results obtained from reference 2, which applies only for saturated free-stream conditions. However, the agreement between the calculated and measured surface temperatures over the fully wet portions of the surface and the formation of ice at the predicted critical region provide sufficient proof that the calculation method is applicable at the 0.8 Mach number condition.

The results obtained with the diamond airfoil for a supersonic free-stream Mach number of approximately 1.35 for pressure altitudes of 25,000 to 42,000 feet are presented in figures 7(c) to (f). For the fully wetted region of the front face, the calculated surface temperatures approximate the measured values very well, the calculated temperature generally being up to 3° F lower than the measured value.

The forward extremity of the observed ice formation was considered as the point corresponding to the point defined in the icing-limit definition, and the free-stream static temperature (icing limit) was determined for the conditions existing at that point from reference 2. The values so obtained are presented in the figure legends together with the experimentally determined free-stream static temperature. The experimental value is from 4° to 8° below the value determined from reference 2. The thermocouples located in the regions corresponding to the observed chordwise position of the ice locations for the most part did not indicate freezing-level temperatures. This discrepancy in the results was apparently caused by the partly wetted nature of the surface and consequent incomplete spanwise development of the ice formation, which were thus not always directly over the thermocouple junctions.

Measurements of the dewpoint of the air stream indicate that the relative humidity of the air stream at the test section varies from a somewhat supersaturated condition at 25,000-feet pressure altitude to a relatively dry condition (relative humidity approximately 15 percent) at 40,000-feet pressure altitude. Evaporation from the droplets in the spray and moisture added to the stream by the air from the spray nozzle tend to increase the humidity locally and would result in a more nearly saturated stream at the model. Because the static temperatures are low for the supersonic condition (from -20° to -50° F), the total water content of the air for complete saturation is low and local saturation may be accomplished by the addition of only small amounts of water vapor.

The similarity of the results at all the altitude conditions indicates that the effect of initial humidity of the ambient air at low static temperature is small. The results presented in the figures showing calculated surface temperatures were obtained by using values of vapor pressure determined from humidity measurements of air samples taken from the plenum chamber. In order to determine the possible effect of change in humidity between the point of measurement and the model, some additional calculations of surface temperature were made with the free

stream considered as at the saturation humidity. For the supersonic free stream, the condition of saturation at the model represents a decrease in the vapor content for the 25,000-foot pressure altitude condition and an increase in vapor content for the 42,000-foot pressure altitude condition. The results of these calculations of the surface temperature show a decrease of less than 0.5° F for the 25,000-foot pressure altitude condition and an increase in temperature of approximately 1.4° F at the 42,000-foot condition, as shown by the dashed line in figure 7(f).

Surface temperature and icing limit - front surface. - Obtaining data on the icing of the forward surfaces of the diamond airfoil necessitated reduction of the air temperature to values considerably below the icing-limit temperature for the rear surfaces. Consequently, icing of the rear surfaces was occurring simultaneously, and it was necessary to obtain the data rapidly before the ice accumulation on the rear surfaces was sufficient to affect the flow field over the entire airfoil. The general icing-limit definition, for a particular point on the body, does not exclude the possibility of the existence of ice elsewhere on the body, if the formation of such ice does not require the inclusion of the heat of fusion term in the calculations for the point in question. The point on the surface corresponding to the conditions of the icing-limit definition is the point which is at a temperature of 32° F and therefore at the newly forming edge of the ice formation.

As the air temperature was reduced, ice on the forward surfaces formed first in the region directly behind the leading edge, and further reduction in the stream temperature caused the ice to extend farther back toward the shoulder. Thus, the point on the surface for which the icing-limit definition applies is the rearward extremity of the ice formation. Figure 8 shows the change in the rearward extent of the icing for two air temperatures at two pressure altitudes. For each of the stream conditions shown, the calculated surface temperature indicates that the region just ahead of the shoulder should be more susceptible to icing than any other part of the forward surface. However, the occurrence of ice formations first near the leading edge, and the rearward movement of the icing with reduction in air temperature may probably be caused by the lower recovery factor near the leading edge and by the high rates of heat transfer and evaporation combined with a value for the ratio of k_e/k_h greater than unity if laminar flow exists in this region. The results of reference 2 apply strictly only to turbulent flow, and the changes in recovery factor and heat and mass transfer that occur in the leading-edge region are not included in the analysis of reference 2.

Values of the measured surface temperature were generally below the freezing point from the foremost thermocouple to the rearward extremity of the front-face ice formation and showed increases to slightly above

the freezing point aft of the ice formation. The calculated surface temperatures over the front face were lowest at midchord, and showed generally increasing values toward the leading-edge region, although consistently below the freezing point over the entire front face. At the experimentally determined location of the point corresponding to the icing-limit conditions, the calculated surface temperatures were generally 2° to 4° F below the freezing-point temperature. The calculations of the icing limit from reference 2 for this region indicate the occurrence of icing at free-stream static temperatures 3° to 10° F higher than were found experimentally.

Circular-Arc Airfoil

Impingement. - On the circular-arc airfoil, direct impingement of the water droplets occurred only over approximately the first 30 percent of chord. Behind the impingement region, surface tension and viscous forces caused the runback water to separate into rivulets. As this investigation was concerned primarily with the temperatures of wet surfaces, it was necessary to provide sufficient runback water to result in nearly fully wetted surfaces behind the limit of impingement, even though high values of liquid-water concentration were required. Although the effect on the surface temperature of increasing the liquid-water concentration is similar for the circular-arc and the diamond airfoils, the smaller droplet impingement area makes the effect of partial wetness of the surface aft of the limit of impingement more apparent for the circular-arc airfoil.

Measured values of the surface temperature for several values of liquid-water concentration at Mach numbers of 0.8 and 1.35 are shown in figure 9 for the circular-arc airfoil. The approximate limit of droplet impingement is included in figure 9(a). The surface temperatures associated with the lower liquid-water concentrations are high because the surfaces aft of the limit of impingement are dry or only partly wet. Values of liquid-water content of approximately 5 grams per cubic meter were required at both Mach number conditions to provide a continuous film of water over the airfoil to the 60-percent-chord position. The reduction in surface temperature with increase in liquid-water content shown in figure 9 occurred only as the rivulets covered a greater percentage of the surface, and an equilibrium temperature was reached when the thermocouple junction became wet. The equilibrium condition is approached for most of the thermocouple locations at liquid-water content of 7.0 grams per cubic meter (fig. 9(a)) at M_0 of 0.8. It was necessary to obtain data only when observation of the airfoil surface indicated that the thermocouples in the region under study were wet. In figure 9 and the figures following, any increase in temperature as a function of chordwise position aft of the midchord position must be considered to be caused by an incompletely wet surface at the thermocouples.

The increase in temperature near the leading edge shown in figure 9(a) ($M_0 = 0.8$) with increase in the value of the liquid-water content from 3.9 to 5.7 grams per cubic meter could be due to the kinetic energy of the droplets, but probably results from the fact that the stream static temperature was higher than the surface temperature. Because the stream humidity was quite low at the subsonic Mach number condition, as discussed in the section Diamond Airfoil, a large evaporative cooling effect on the model existed, with the result that the icing-limit condition occurred at high values of the stream static temperature. Thus, the spray was warm compared with the surface. At the high liquid-water concentrations, a finite time and distance were required for the evaporation at the surface of the water film to cool the remaining water to the equilibrium surface temperature, with the result that the process was incomplete at the forward stations. The reasons presented for the increase in temperature near the leading edge at the 0.8 Mach number condition are substantiated by the 1.35 Mach number results of figure 9(b). The increase in temperature is less at the higher Mach number and, therefore, is probably not a result of the kinetic energy of the droplets. An estimate of the cooling caused by the expansion of the spray-nozzle air and the evaporation from the droplets (from the results presented in ref. 8) indicates that the drops would approach the stream static temperature, which is lower than the surface temperature, and thus would not raise the leading-edge surface temperature at the 1.35 Mach number condition.

Surface temperature and icing limit. - Figure 10 presents measured surface temperatures obtained with the circular-arc airfoil, together with calculated surface temperatures ($r = 0.88$) and observed ice-formation locations for Mach numbers of 0.6, 0.8, and 1.35 at pressure altitudes from 25,000 to 40,000 feet. Included in each figure for the 30,000-foot pressure altitude condition is the surface temperature calculated with values of the recovery factor corresponding approximately to the variation with chordwise position shown in figure 5 (figs. 10(b), (e), and (h)).

The results shown in figures 10(a) to (f) are for subsonic free-stream Mach number conditions. The minimum calculated surface temperature occurs at or near the midchord position. However, ice was observed to form first in the region just behind the leading edge, and the minimum value of the measured surface temperature also occurred in this region. Near the leading edge, the existence of a laminar-flow region with the resulting high convective heat-transfer and evaporation rates, combined with a value greater than unity for the ratio of the evaporation and heat-transfer coefficient, probably accounts for most of the difference between the measured surface temperature values and the surface temperatures calculated by equation (1) with values for the recovery factor as a function of chordwise position. Observation of the airfoil during the initial period of ice formation disclosed that, at the higher altitude conditions, ice crystals formed in the water film, slid back along the

surface, and disappeared apparently from melting rather than from blow-off. Because the humidity of the air stream was very low and the amount of water vapor required for saturation was not negligible, the subsonic results obtained with the circular-arc airfoil model may not be compared directly with the free-stream icing-limit temperature results of reference 2, which apply only if the air stream is saturated. However, the surface temperatures calculated with the method employed in reference 2, but with values of the vapor pressure corresponding to the humidity measurements made during the experiment, show reasonable agreement with measured temperatures over the forward regions of the airfoil (figs. 10(a) to (f)).

The results obtained for several pressure altitudes at a Mach number of 1.35 are shown in figures 10(g) to (j). Ice was observed to form first in the region just behind the midchord position. Measured and calculated surface temperatures both show agreement as to the location of the critical region for the initial formation of ice. Surface temperatures very near the freezing point were measured in the vicinity of the ice location at each of the altitude conditions. Calculated surface temperatures approximately 4° F below the measured temperature were obtained in the critical region. The trend of the measured surface temperatures to values lower than the calculated temperature in the leading-edge region is apparent in figures 10(g) to (j) as it was in previous figures for both the diamond and circular-arc airfoil models. The icing-limit temperatures $t_{0,c}$ based on the location of the ice, included in the figure legends, show that reference 2 predicts the formation of ice at temperatures from 7° to 12° F higher than the experimentally determined limiting temperature. The occurrence of the ice formation near the reflected-shock intersection and the slope of the calculated surface temperature curve indicate that the ice might have formed nearer the trailing edge and at a higher stream temperature if the shock had not been present.

General Comparison of Calculated and Experimental Results

The experimental data presented herein show that the results of references 1 to 3 may be applied generally over a considerable range of pressure altitude and Mach number conditions to give reasonably good prediction of the wet-surface temperature or the ambient-air temperature that will result in icing at any point on a body. Comparison of figures 7 to 10 shows that calculated wet-surface temperatures for all but the foremost regions of the airfoils were generally 2° to 4° F below the measured surface temperatures in the fully wetted areas of the airfoils. In addition, predictions made from reference 2 of the maximum ambient-air temperature that will result in icing were indicated to be conservative in every case (icing of the surface occurred at a lower maximum air temperature than indicated from the results of ref. 2). Although these results show sufficiently good agreement to verify the use of the analytical

method and results of reference 2, it is of interest that the calculated values of surface temperature for all but the leading-edge region are consistently below the measured values. Observed icing usually coincided with values of the measured surface temperature very near the freezing point.

Factors that would result in higher values of the measured surface temperature than would be indicated by the calculations are:

(1) Transfer of heat by conduction through model from tunnel walls and unwetted portions of model

(2) Heat gained by radiation from surrounding surfaces

(3) Heat due to kinetic energy of droplets

(4) Heat gained from droplets formed from room-temperature water that did not reach equilibrium with static air temperatures at supersonic Mach number condition

(5) High free-stream static temperature and spray temperature at icing-limit condition for subsonic conditions as a result of low stream humidity

The conduction of heat through the model was minimized by the use of the plastic insert of low thermal conductivity and by the fact that the plastic material was not bonded to the metal portions of the model. For the temperature differences between the model and the surroundings that existed during the experiments, the heat gained by radiation is so slight as to be of no consequence. The effect of items (3) to (5) would be higher values of the surface temperature in the impingement region as a function of the liquid-water content of the air. A discussion of these factors for the case of the circular-arc airfoil was included in the discussion of that airfoil; and the results for the diamond airfoil would be similar, except that the impingement region covers the entire forward-facing surfaces. An additional factor that reduced the temperature reading nearest the leading edge by approximately 1° F was the spray-nozzle air jet, which was generally at a lower total temperature than the stream. The effect elsewhere on the model was negligible.

In addition to the factors discussed in the preceding paragraph that have an effect on the measured surface temperature, there are several aspects of the analytical method that could also contribute to the differences between measured and calculated values. In the analysis used herein and for references 1 to 3, the assumption has been made that in the region just outside the boundary layer the air may become supersaturated with water vapor but condensation of the vapor does not occur. Hardy (ref. 3) discusses the possibility that such condensation may actually

occur, however. If such is the case, then the value of the specific heat used to determine the local static temperature must be altered commensurate with the rate of change of phase of the vapor. Calculations made using the experimental data for the conditions resulting in the highest degree of saturation of the free stream and considering complete and instantaneous condensation of all water vapor in excess of saturation resulted in a small (0.5° F) increase in the value of the calculated surface temperature at the first thermocouple station and a 1.1° F increase just after the midchord position.

The value of unity for the ratio of the coefficients of mass and heat transfer has been widely used and accepted, but exact agreement has not been shown experimentally. Thus the use of the value of unity for this relation in equations (1) and (2) may also contribute to the consistent difference between measured and calculated values.

The analytical determination of the free-stream static temperature at the icing limit is somewhat more sensitive to the value used for the ratio k_e/k_h than is the analytical determination of the surface temperature. For example, a 10-percent change in the value of the ratio at M_0 of 1.35 and pressure altitude of 30,000 feet would cause a change of approximately 3.5° F in the value of $t_{0,c}$ that would be obtained by the method of reference 2, and would cause a change of approximately 1.5° F in the values of the calculated surface temperatures. A reduction in the value of the ratio causes the calculated values of $t_{0,c}$ and t_s to approach the experimental values.

SUMMARY OF RESULTS

The twofold experimental investigations to determine the wet-surface temperatures on bodies in subsonic and supersonic air streams, together with determination of the stream conditions for which ice will just start to form on the surfaces, yielded the following results:

1. Measured values of the wet-surface temperature were consistently 2° to 4° F higher than were calculated with equations given in references 1 and 2 together with experimental free-stream static temperatures for all but the foremost part of the fully wetted regions of the models.

2. Agreement between the experimental and analytical results shows that the results of references 1 and 2 are sufficiently accurate to be applied generally. Calculated values of the icing-limit conditions were consistently conservative compared with the experimental results, predicting the formation of ice at values of ambient-air temperature up to 12° F higher and at an average value 7° F higher than the values determined by experiment.

3. The locations of analytically determined regions on the airfoil susceptible to the initial formation of ice were generally substantiated by experiment. An exception was observed in the case of the circular-arc airfoil model at subsonic airspeeds, for which the region of initial ice formation occurred near the leading edge instead of at the midchord region as predicted analytically.

Lewis Flight Propulsion Laboratory
National Advisory Committee for Aeronautics
Cleveland, Ohio, November 18, 1954

REFERENCES

1. Callaghan, Edmund E., and Serafini, John S.: Analytical Investigation of Icing Limit for Diamond-Shaped Airfoil in Transonic and Supersonic Flow. NACA TN 2861, 1953.

2. Callaghan, Edmund E., and Serafini, John S.: A Method for Rapid Determination of the Icing Limit of a Body in Terms of the Stream Conditions. NACA TN 2914, 1953.

3. Hardy, J. K.: Kinetic Temperature of Wet Surfaces - A Method of Calculating the Amount of Alcohol Required to Prevent Ice, and the Derivation of the Psychrometric Equation. NACA WR A-8, 1945. (Supersedes NACA ARR 5G13.)

4. Callaghan, Edmund E.: Analogy Between Mass and Heat Transfer with Turbulent Flow. NACA TN 3045, 1953.

5. Coles, Willard D., and Ruggeri, Robert S.: Experimental Investigation of Sublimation of Ice at Subsonic and Supersonic Speeds and Its Relation to Heat Transfer. NACA TN 3104, 1954.

6. Nukiyama, Shiro, and Tanasawa, Yasushi (E. Hope, trans.): Experiments on the Atomization of Liquids in an Air Stream. Rep. No. 4, The Influence of the Characteristics of the Liquid on the Diameter of the Atomized Droplets. Defence Res. Board, Dept. Nat. Defence, Ottawa (Canada), Mar. 18, 1950. (Translated from Trans. Soc. Mech. Eng. (Japan), vol. 5, no. 18, Feb. 1939, pp. 68-75.)

7. Kaye, Joseph: Survey of Friction Coefficients, Recovery Factors, and Heat-Transfer Coefficients for Supersonic Flow. Tech. Rep. No. 6418-5, Dept. Mech. Eng. and Div. Ind. Cooperation, M.I.T., Oct. 1, 1953. (Office Naval Res. Contract N5ori-07805, NR-061-028, D.I.C. Proj. No. 6418.)

8. Lowell, Herman H.: Maximum Evaporation Rates of Water Droplets Approaching Obstacles in the Atmosphere under Icing Conditions. NACA TN 3024, 1953.

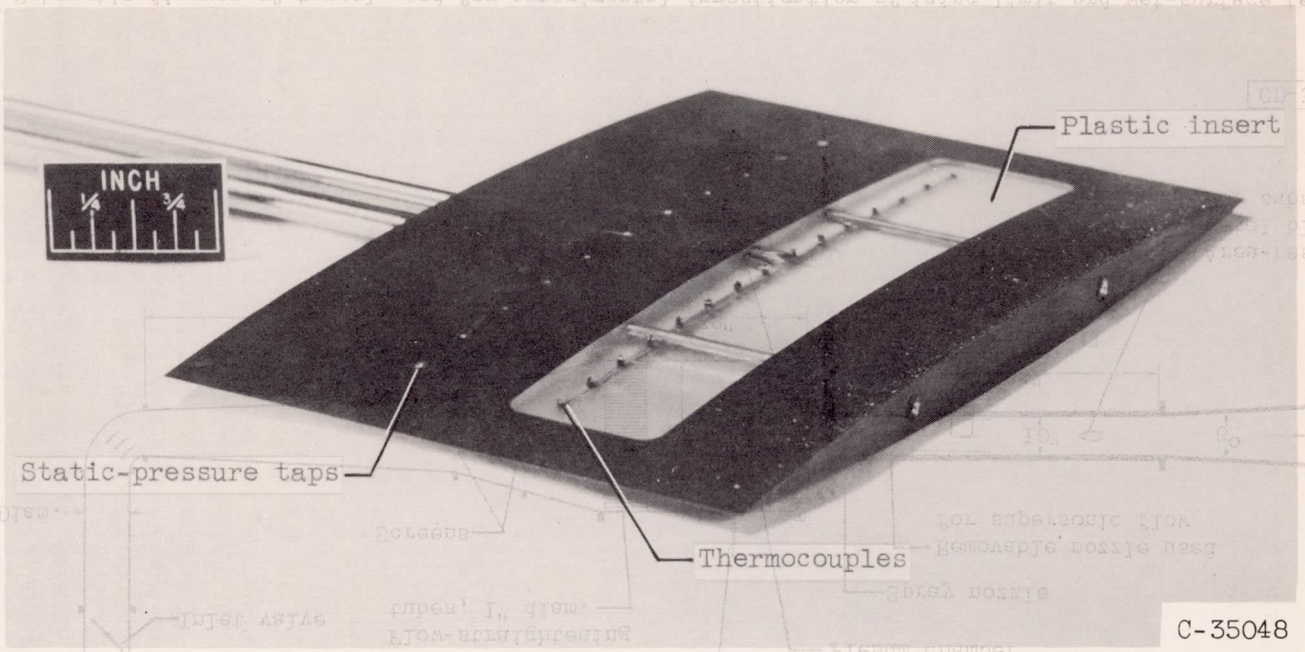

Figure 1. - Circular-arc airfoil model.

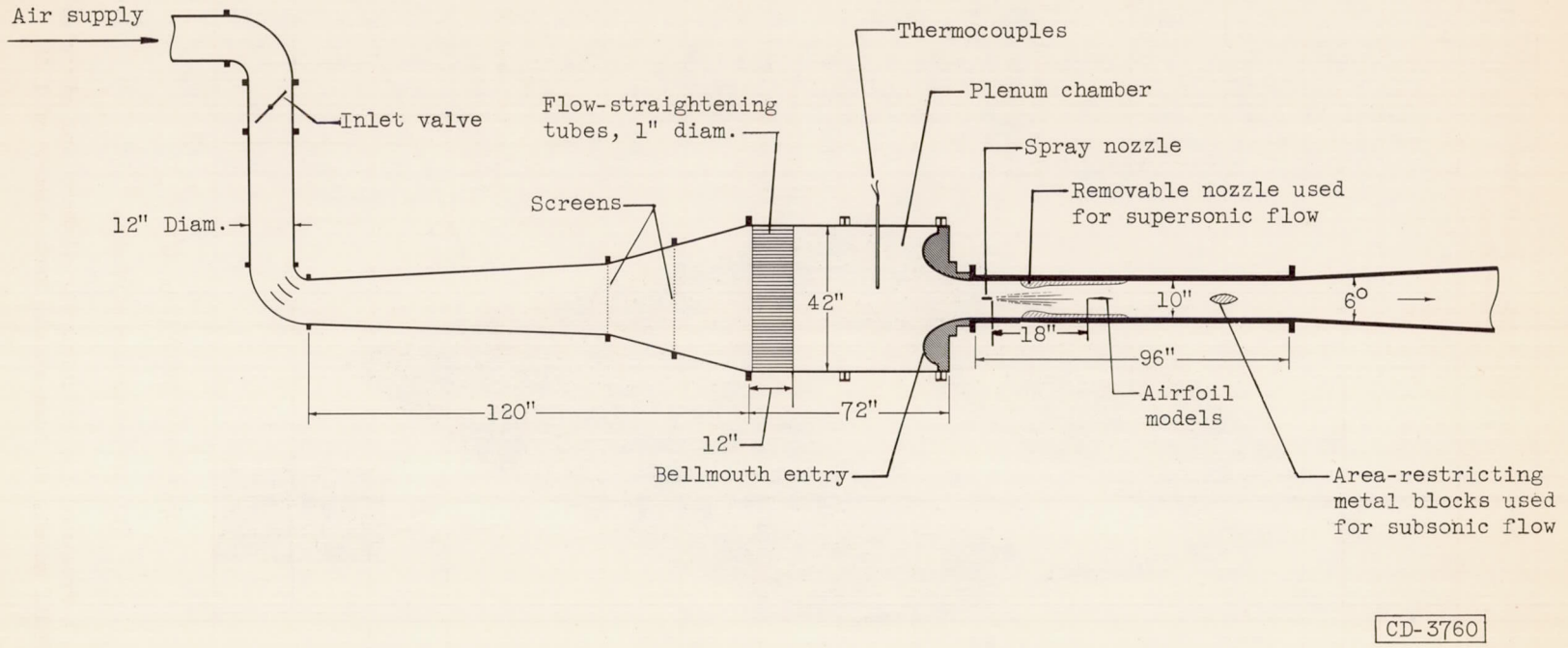

Figure 2. - Schematic diagram of tunnel used for experimental investigation of icing limit and wet-surface temperature.

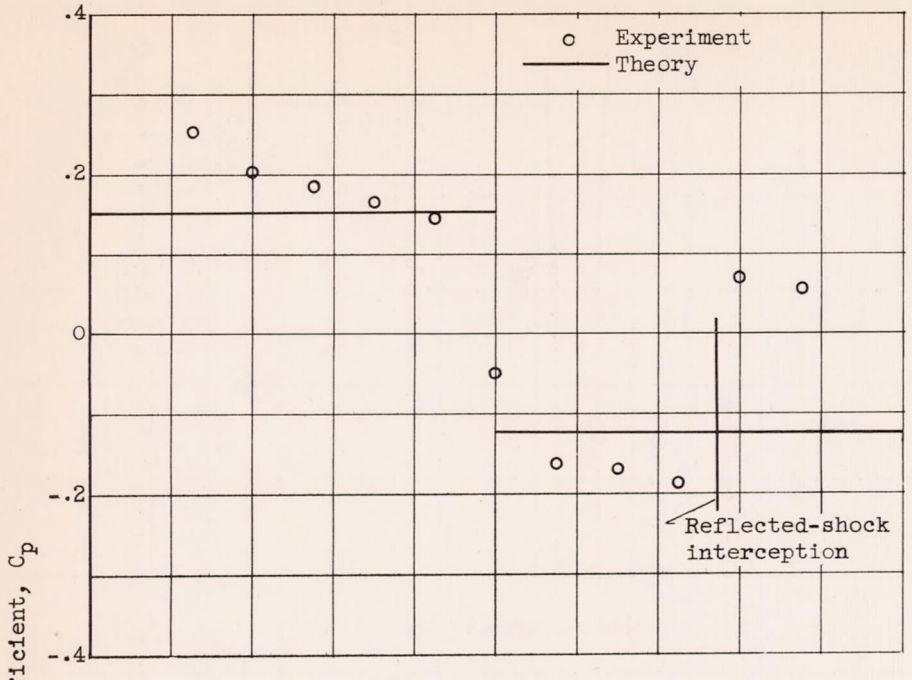

(a) Diamond airfoil.

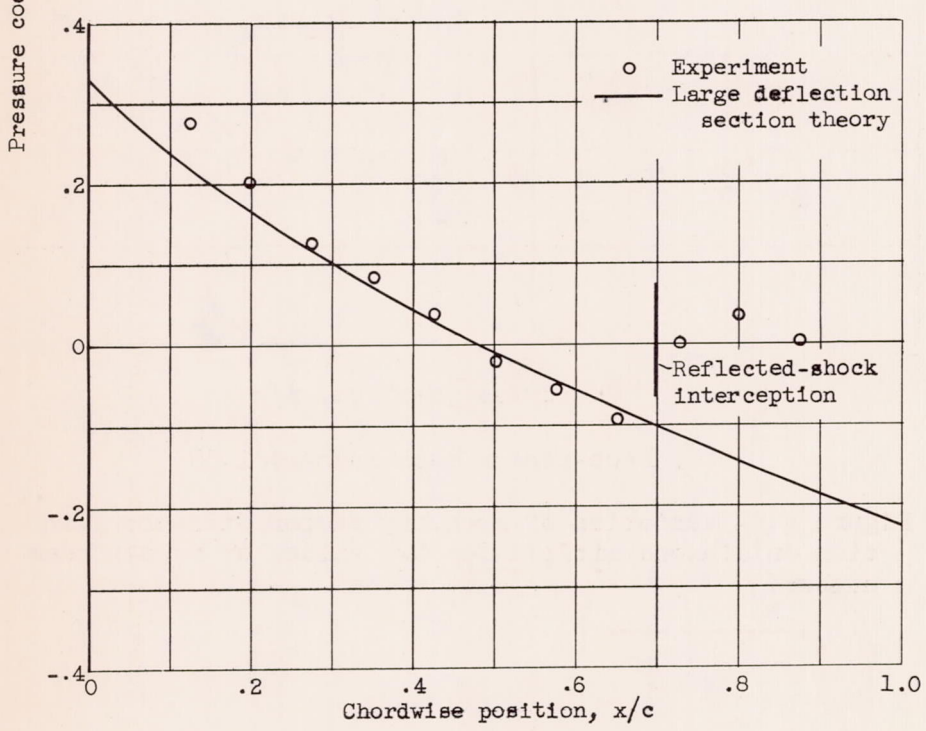

(b) Circular-arc airfoil.

Figure 3. - Pressure distribution for diamond and circular-arc airfoil models at free-stream Mach number of 1.35.

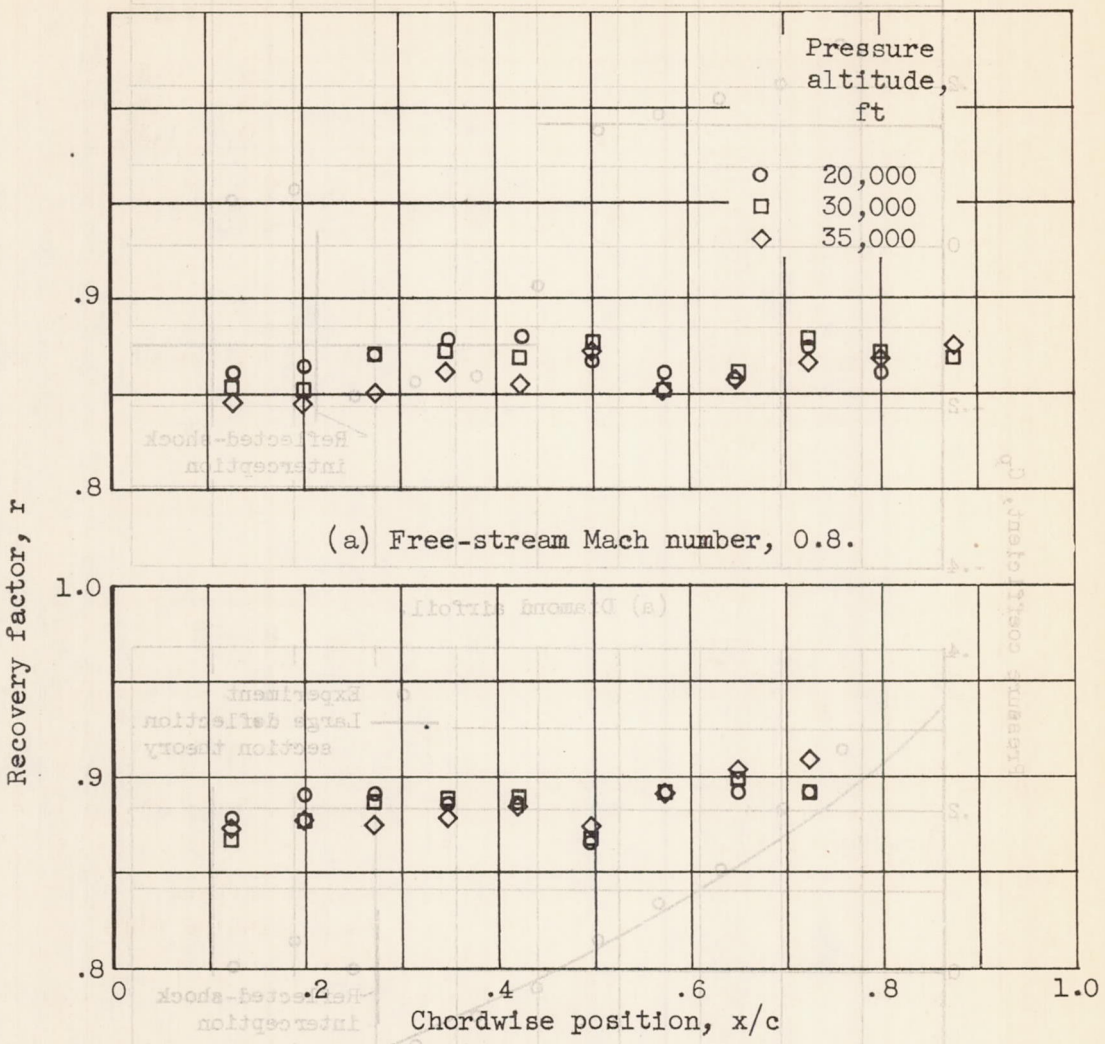

(a) Free-stream Mach number, 0.8.

(b) Free-stream Mach number, 1.35.

Figure 4. - Variation of recovery factor with chordwise position on diamond airfoil for two values of free-stream Mach number.

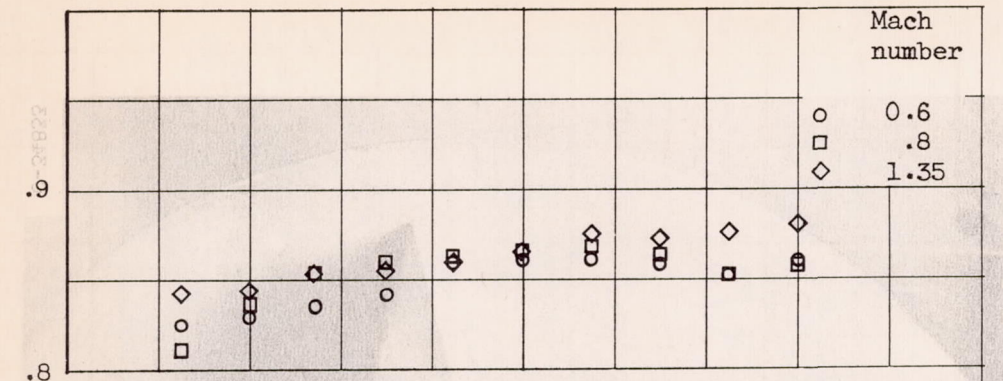

(a) Pressure altitude, 30,000 feet at several values of free-stream Mach number.

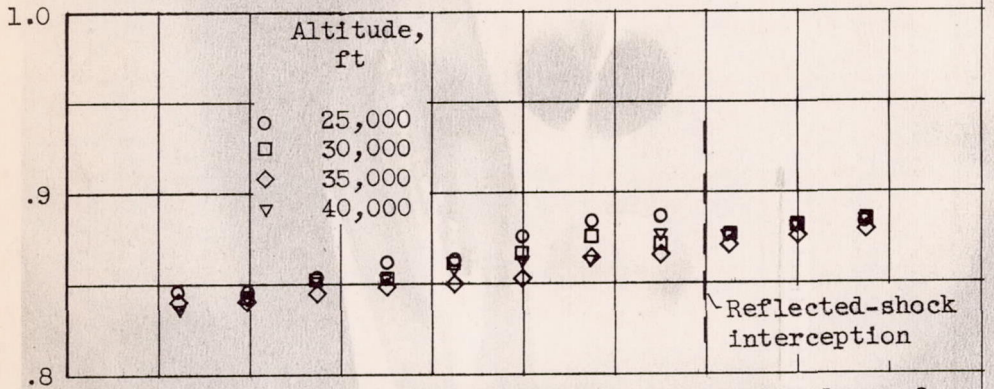

(b) Free-stream Mach number, 1.35, at several values of pressure altitude.

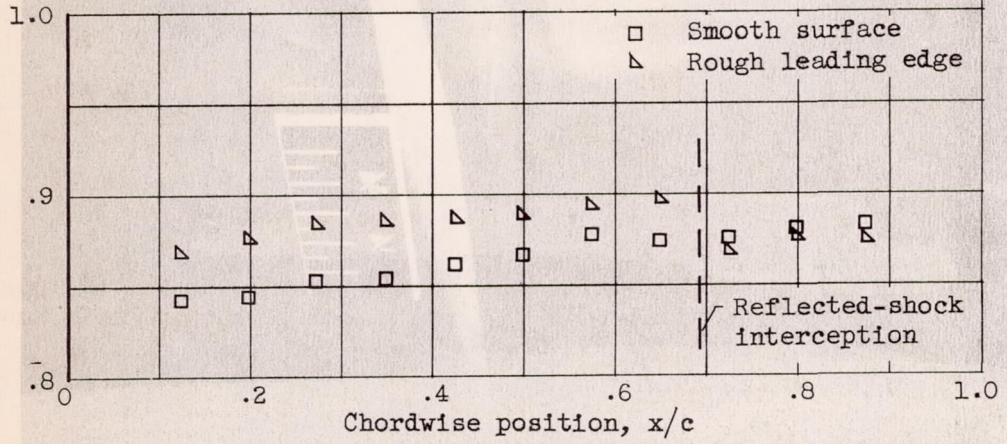

(c) Effect of roughness at leading edge at free-stream Mach number of 1.35 and pressure altitude of 30,000 feet.

Figure 5. - Variation of recovery factor with chordwise position on circular-arc airfoil.

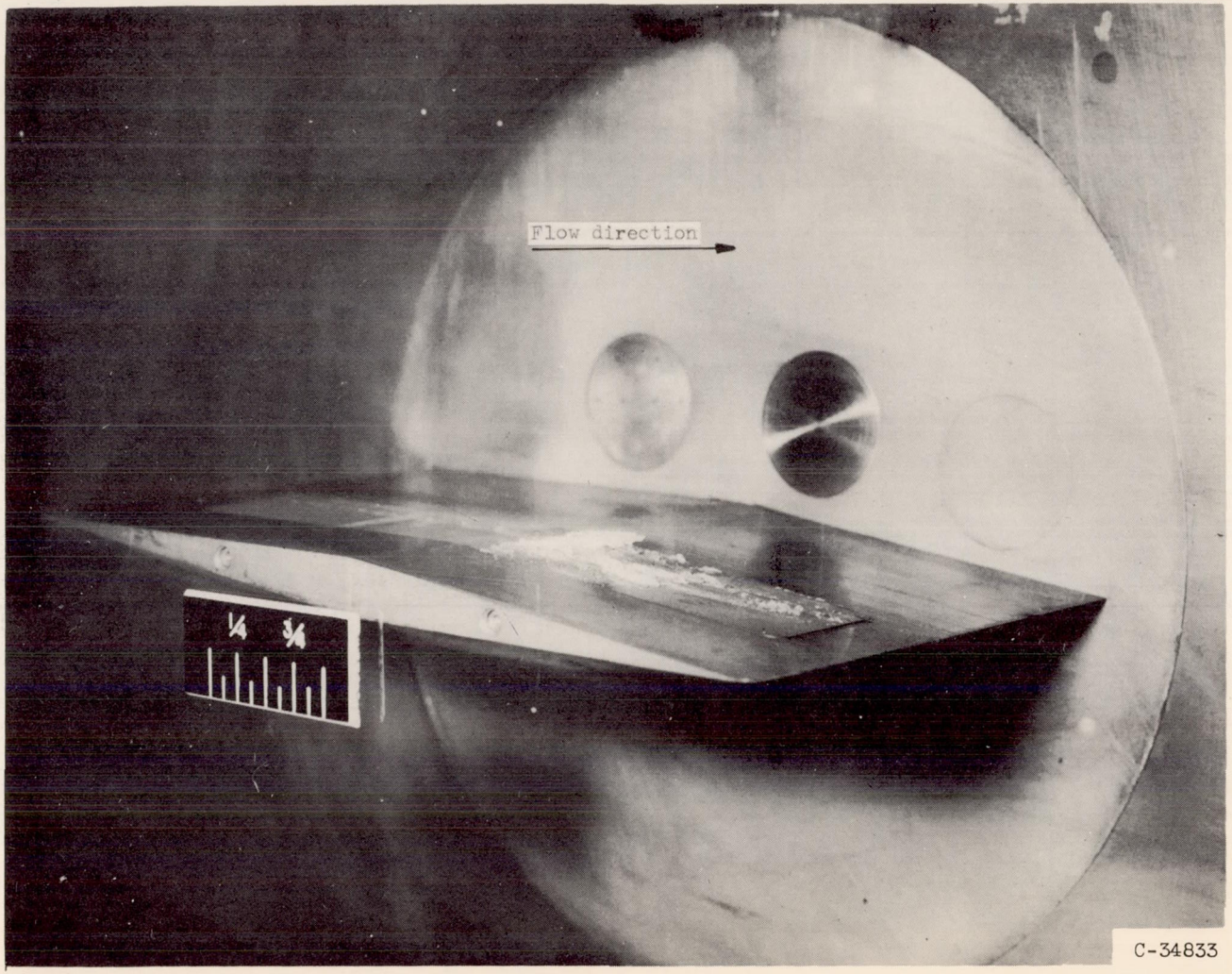

Figure 6. - Diamond airfoil model in tunnel, showing ice formed at Mach 1.35 on top surface behind shoulder.

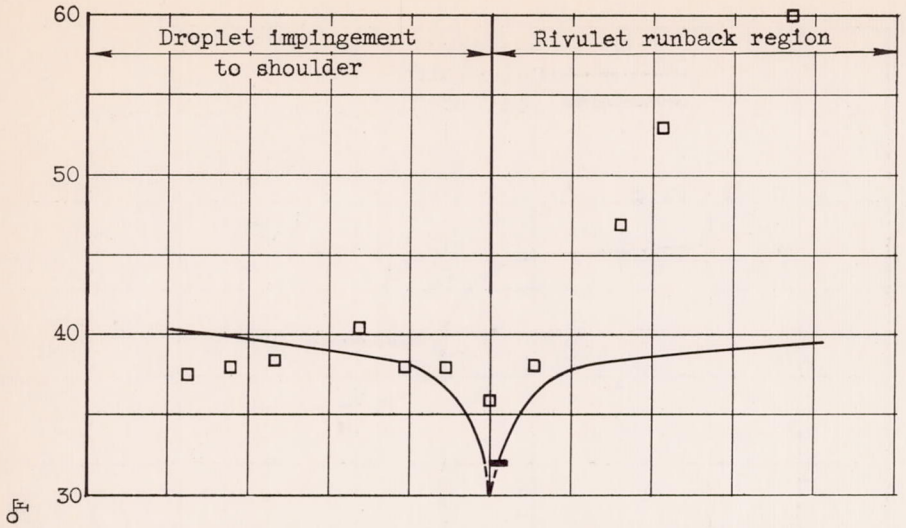

(a) Free-stream Mach number, 0.8; pressure altitude, 30,000 feet. Free-stream static temperature t_0 (exp.), 69.1° F; $t_{0,c}$ (ref. 2), not applicable.

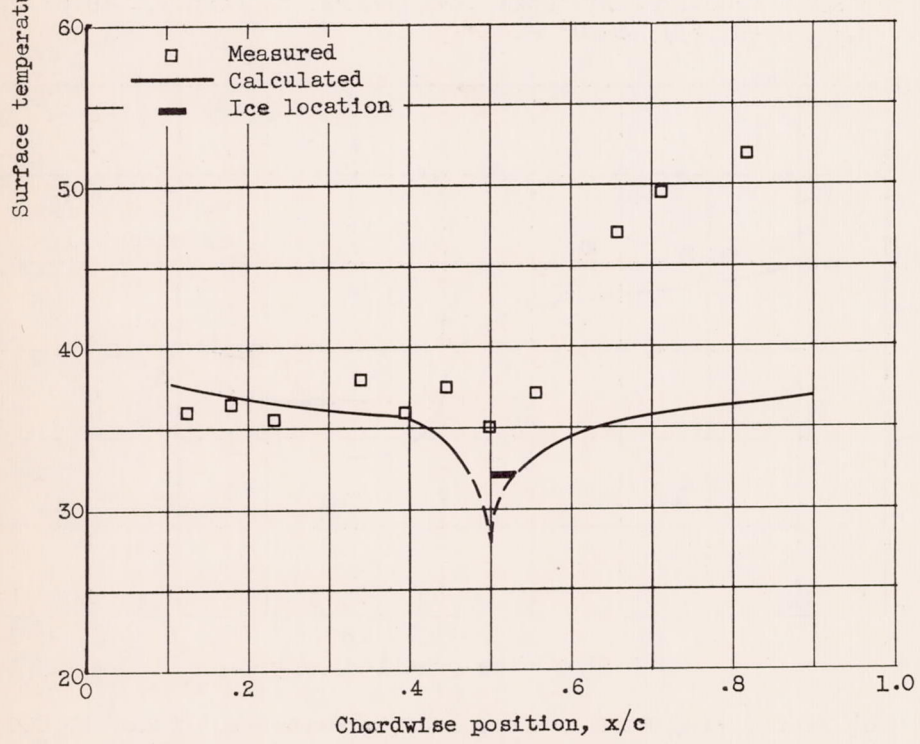

(b) Free-stream Mach number, 0.8; pressure altitude, 35,000 feet. Free-stream static temperature t_0 (exp.), 82.8° F; $t_{0,c}$ (ref. 2), not applicable.

Figure 7. - Surface temperatures on diamond airfoil at icing limit.

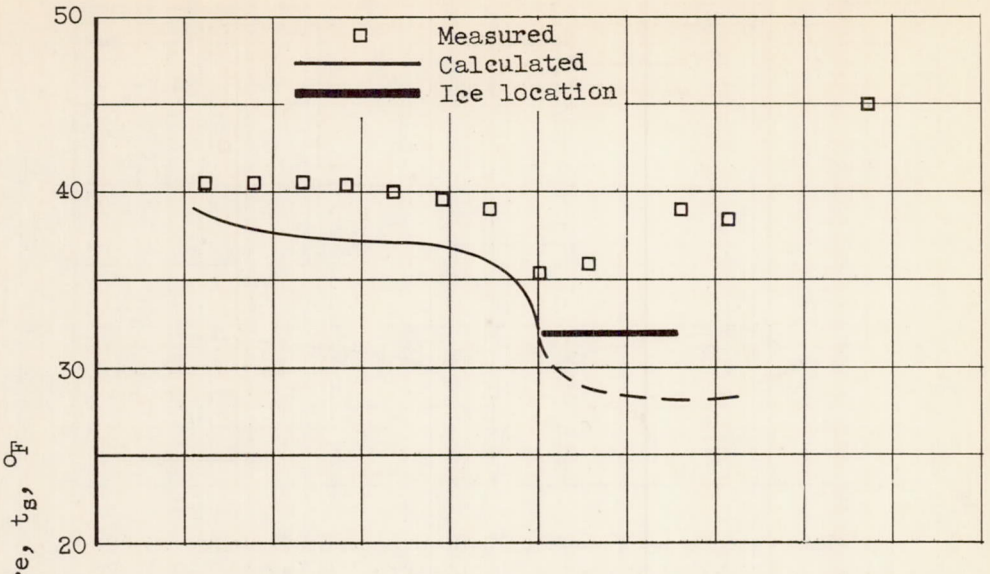

(c) Free-stream Mach number, 1.35; pressure altitude, 25,000 feet. Free-stream static temperature t_0 (exp.), -49.8° F; $t_{0,c}$ (ref. 2), -45.9° F.

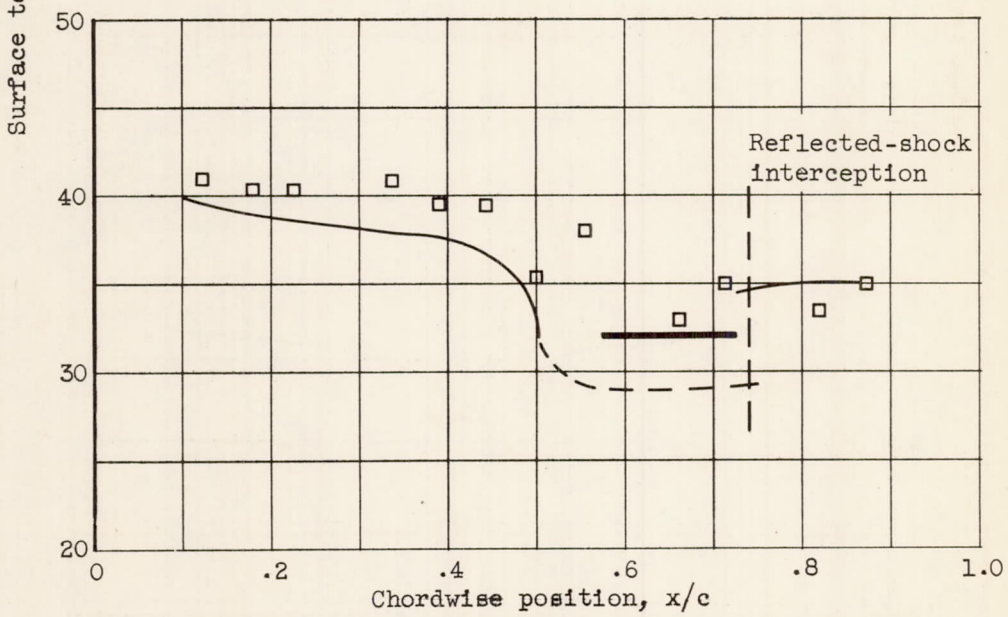

(d) Free-stream Mach number, 1.35; pressure altitude, 30,000 feet. Free-stream static temperature t_0 (exp.), -38.4° F; $t_{0,c}$ (ref. 2), -31.1° F.

Figure 7. - Continued. Surface temperatures on diamond airfoil at icing limit.

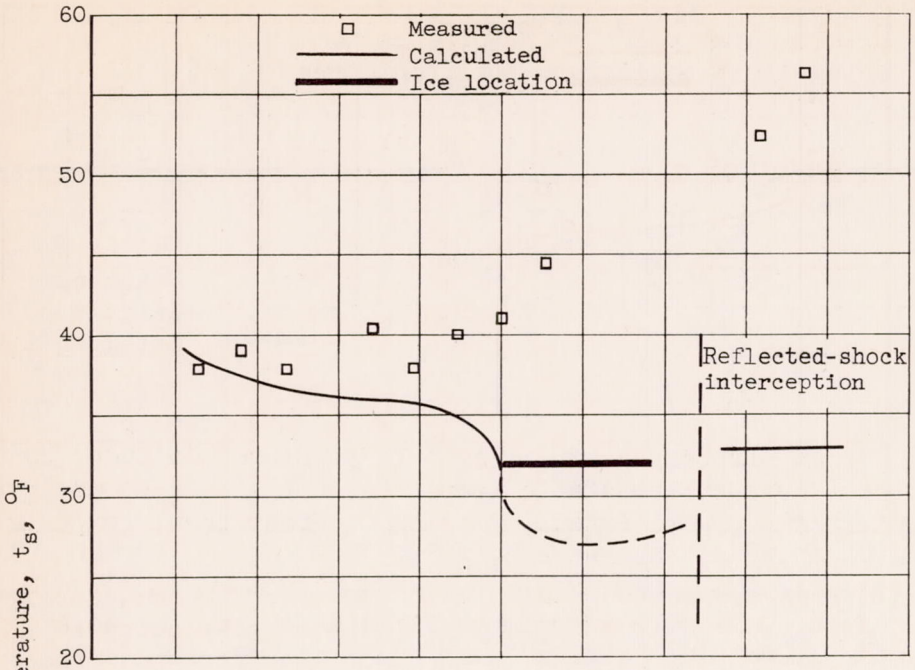

(e) Free-stream Mach number, 1.35; pressure altitude, 35,000 feet. Free-stream static temperature t_0 (exp.), -28.9° F; $t_{0,c}$ (ref. 2), -22.8° F.

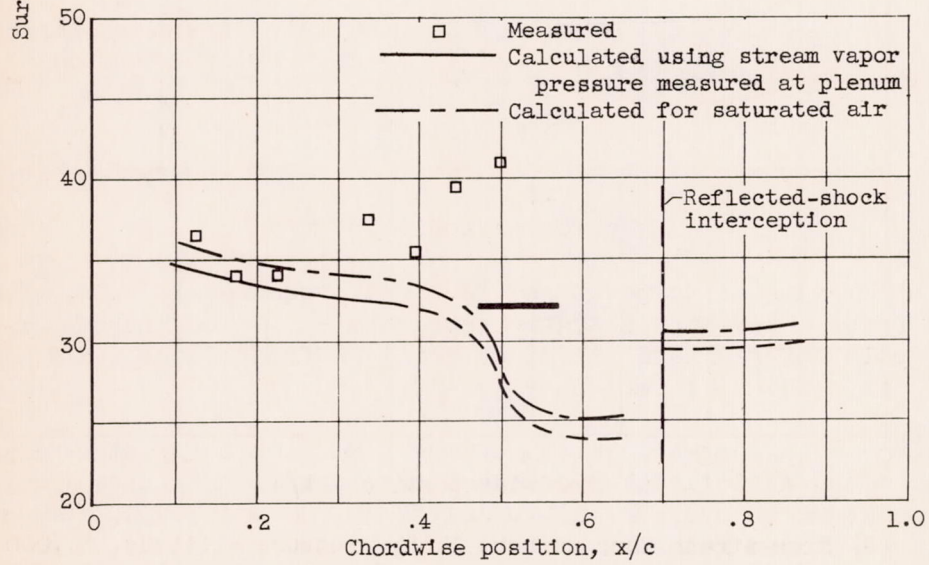

(f) Free-stream Mach number, 1.35; pressure altitude, 42,000 feet. Free-stream static temperature t_0 (exp.), -22.4° F; $t_{0,c}$ (ref. 2), -17.8° F.

Figure 7. - Concluded. Surface temperatures on diamond airfoil at icing limit.

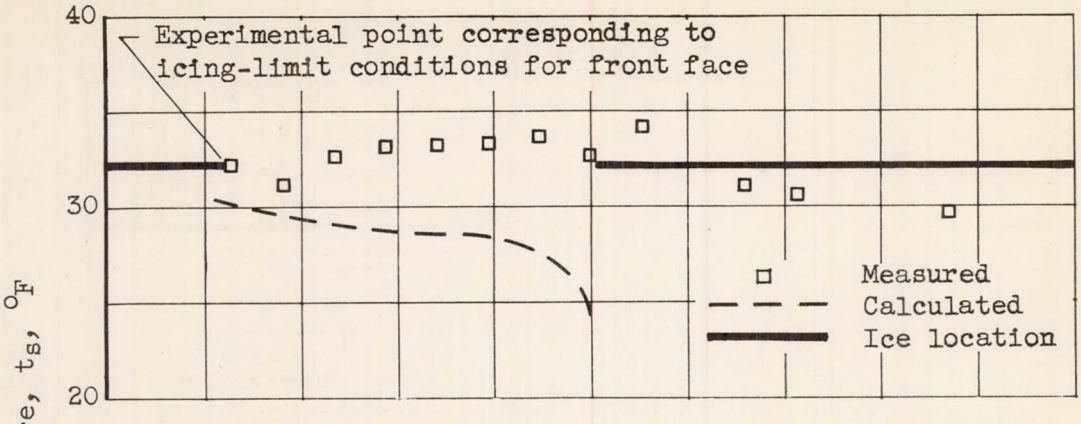

(a) Plenum air temperature, 74.2° F; pressure altitude, 25,000 feet. Free-stream static temperature t_0 corresponding to point of rearward extent of icing on front face: experimental, -65.2° F; reference 2, -62.0° F.

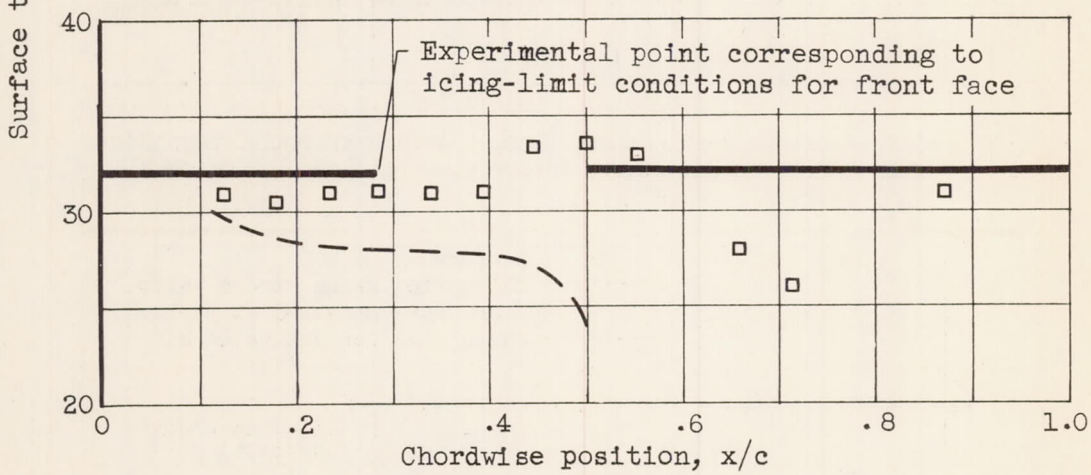

(b) Plenum air temperature, 72.4° F; pressure altitude, 25,000 feet. Free-stream static temperature t_0 corresponding to point of rearward extent of icing on front face: experimental, -66.6° F; reference 2, -59.2° F.

Figure 8. - Rearward extent of ice formation on front face of diamond airfoil for two values of stagnation (plenum air) temperature at pressure altitudes of 25,000 and 30,000 feet and free-stream Mach number of 1.35.

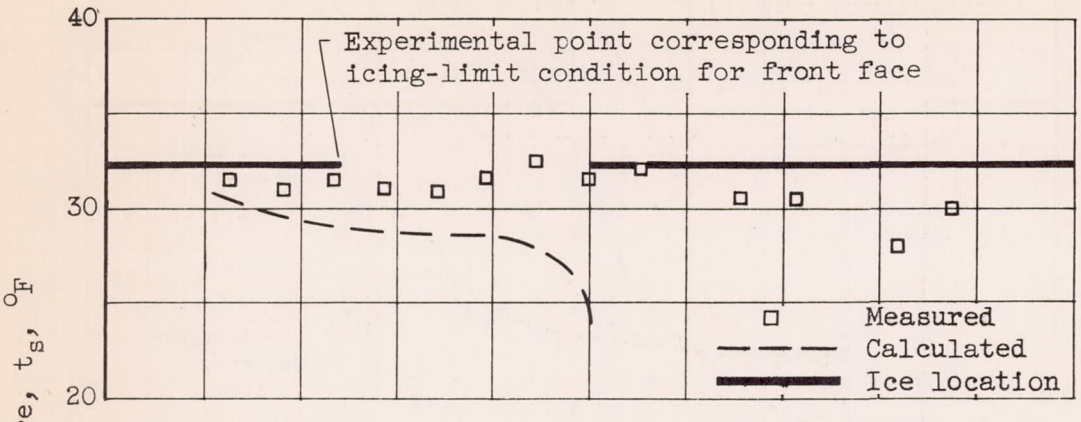

(c) Plenum air temperature, 83.4° F; pressure altitude, 30,000 feet. Free-stream static temperature t_0 corresponding to point of rearward extent of icing on front face: experimental, -57.6° F; reference 2, -50.4° F.

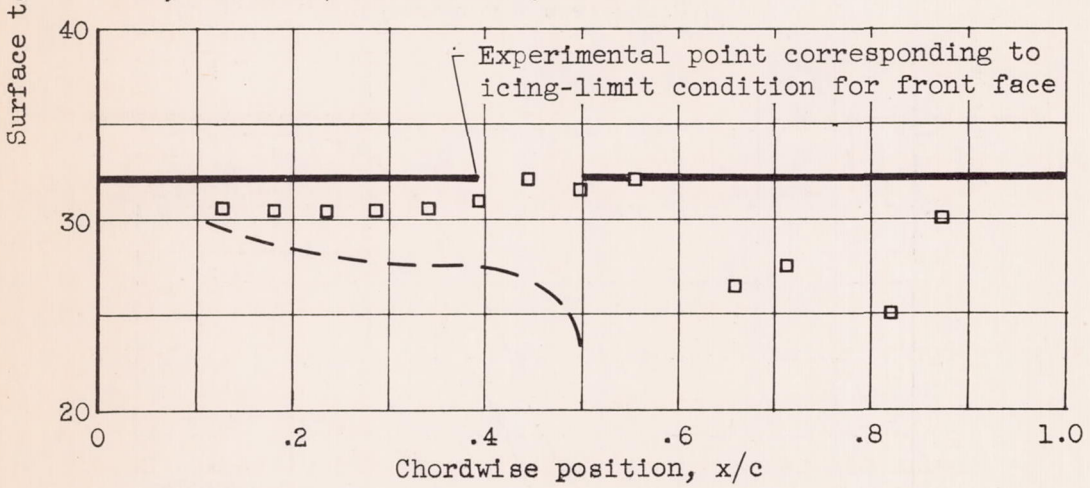

(d) Plenum air temperature, 80.5° F; pressure altitude, 30,000 feet. Free-stream static temperature t_0 corresponding to point of rearward extent of icing on front face: experimental, -60.6° F; reference 2, -51.2° F.

Figure 8. - Concluded. Rearward extent of ice formation on front face of diamond airfoil for two values of stagnation (plenum air) temperature at pressure altitudes of 25,000 and 30,000 feet and free-stream Mach number of 1.35.

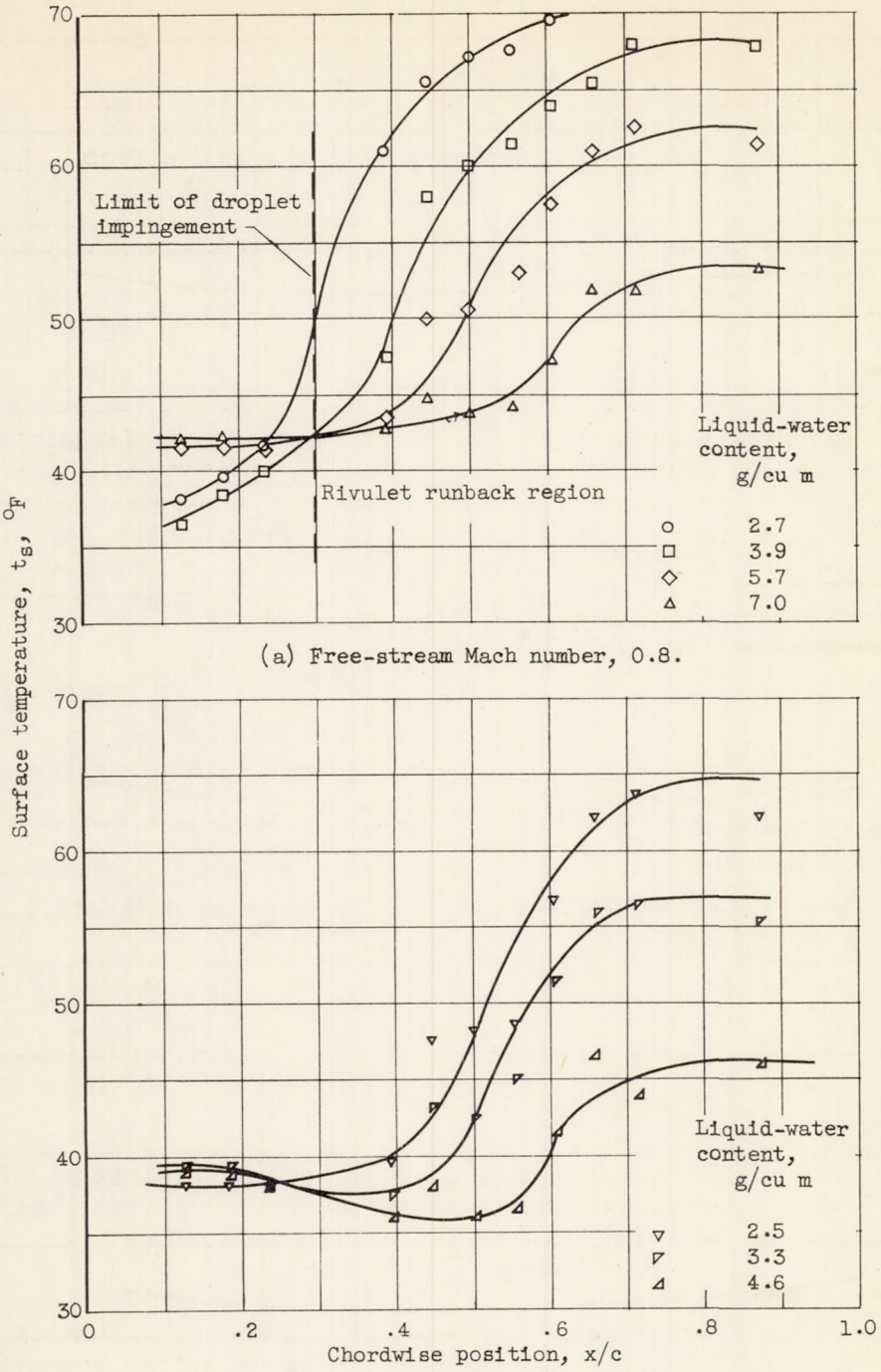

(a) Free-stream Mach number, 0.8.

(b) Free-stream Mach number, 1.35.

Figure 9. - Variation of measured wet-surface temperature on circular-arc airfoil for several values of liquid-water content at two Mach number conditions.

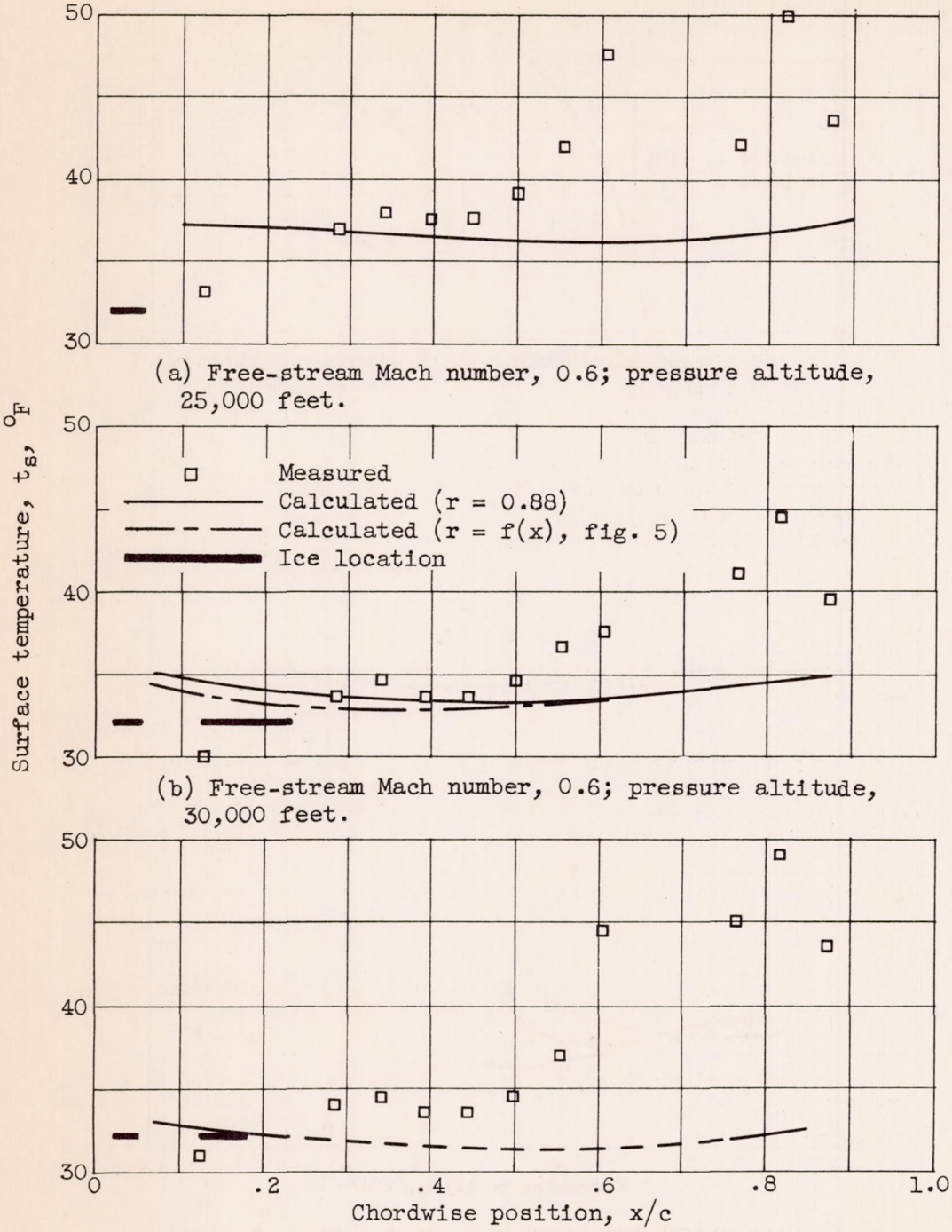

(a) Free-stream Mach number, 0.6; pressure altitude, 25,000 feet.

(b) Free-stream Mach number, 0.6; pressure altitude, 30,000 feet.

(c) Free-stream Mach number, 0.6; pressure altitude, 35,000 feet.

Figure 10. - Surface temperatures on circular-arc airfoil at icing limit.

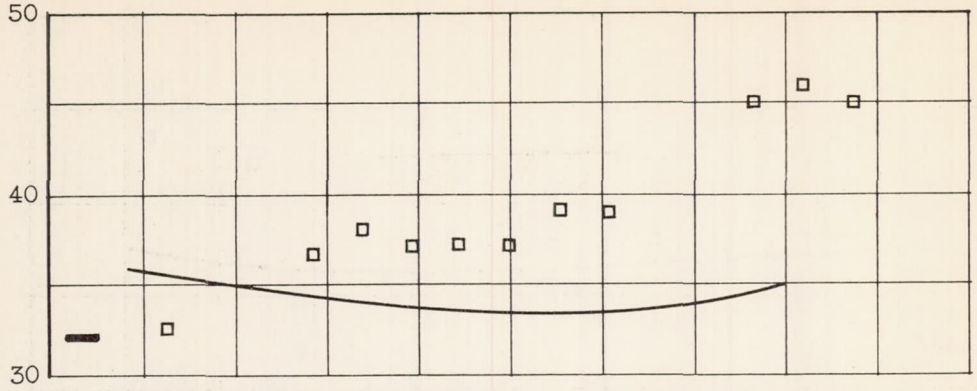

(d) Free-stream Mach number, 0.8; pressure altitude, 25,000 feet.

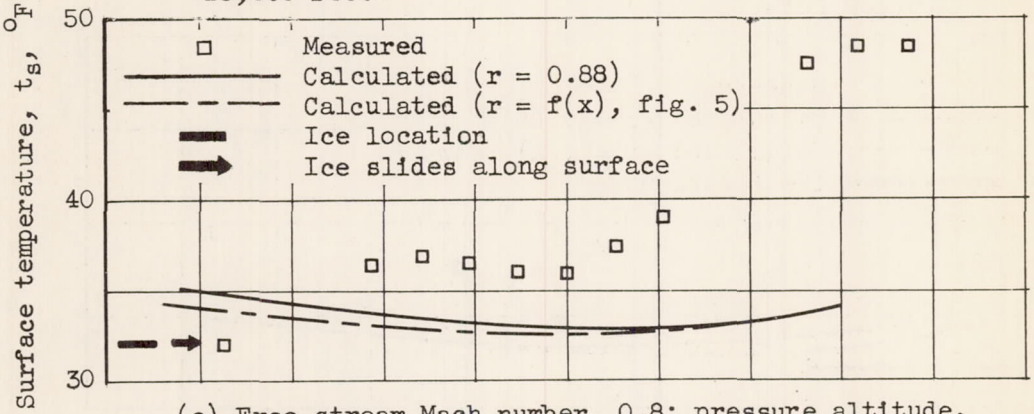

(e) Free-stream Mach number, 0.8; pressure altitude, 30,000 feet.

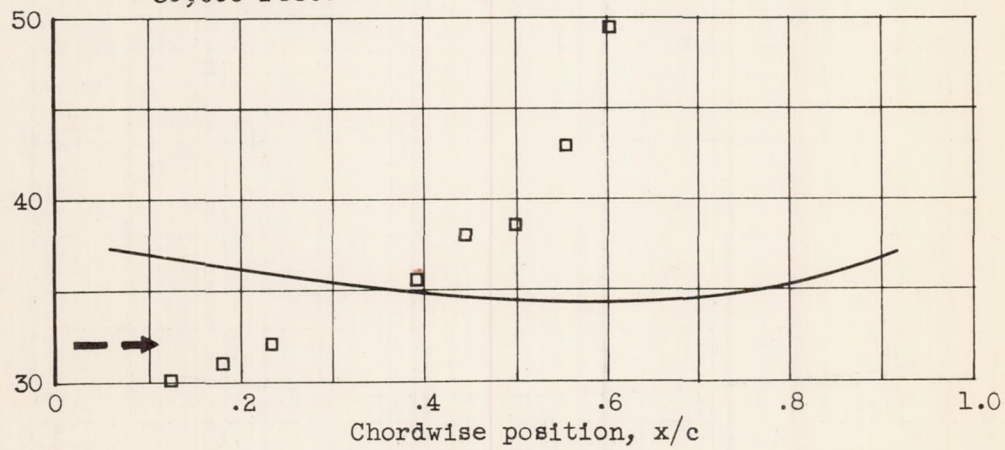

(f) Free-stream Mach number, 0.8; pressure altitude, 35,000 feet.

Figure 10. - Continued. Surface temperature on circular-arc airfoil at icing limit.

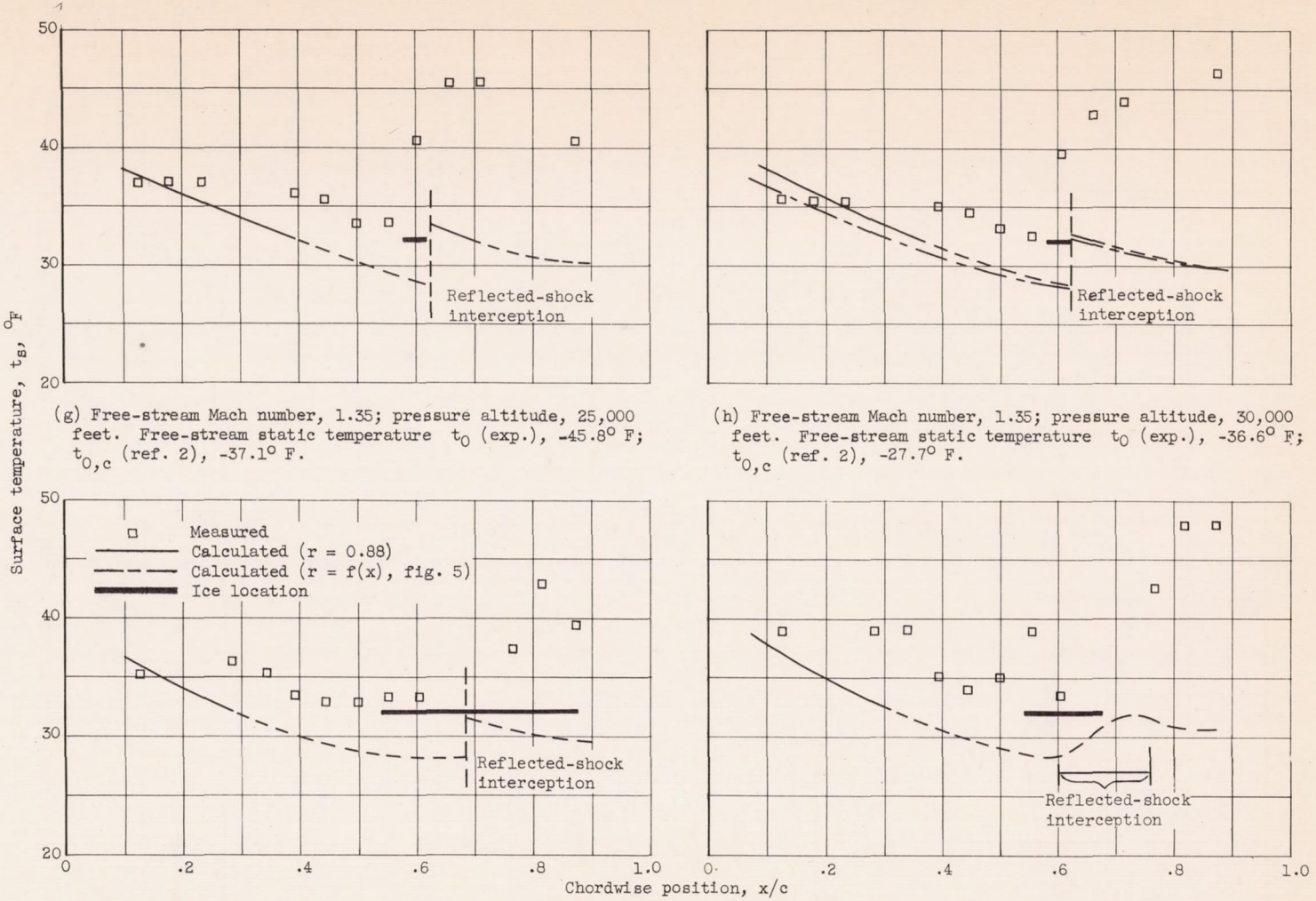

(g) Free-stream Mach number, 1.35; pressure altitude, 25,000 feet. Free-stream static temperature t_0 (exp.), -45.8° F; $t_{0,c}$ (ref. 2), -37.1° F.

(h) Free-stream Mach number, 1.35; pressure altitude, 30,000 feet. Free-stream static temperature t_0 (exp.), -36.6° F; $t_{0,c}$ (ref. 2), -27.7° F.

(i) Free-stream Mach number, 1.35; pressure altitude, 35,000 feet. Free-stream static temperature t_0 (exp.), -39.6° F; $t_{0,c}$ (ref. 2), -27.9° F.

(j) Free-stream Mach number, 1.35; pressure altitude, 40,000 feet. Free-stream static temperature t_0 (exp.), -18.1° F; $t_{0,c}$ (ref. 2), -8.2° F.

Figure 10. - Concluded. Surface temperatures on circular-arc airfoil at icing limit.